PROCEEDINGS OF SCIENCE

Spin and parity assignments for ^{94,95}Mo neutron resonances measured with the DANCE array

G.E. Mitchell*[a], U. Agvaanluvsan[b], J.A. Becker[b], F. Bečvář[c], T.A. Bredeweg[d], R. Haight[d], M. Krtička[c], J.M. O'Donnell[d], W. Parker[b], R. Reifarth[d], R.S. Rundberg[d], E.I. Sharapov[e], S. Sheets[a,b], I. Tomandl[f], J.L. Ullmann[d], D. Vieira[d], J.M. Wouters[d], J.B. Wilhelmy[d], C.Y. Wu[b]

[a] *North Carolina State University, Raleigh, NC 27695*
and Triangle Universities Nuclear Laboratory, Durham, NC 27708
[b] *Lawrence Livermore National Laboratory, Livermore, California 94550, USA*
[c] *Faculty of Mathematics and Physics, Charles University in Prague,*
V Holešovičkách 2, CZ-180 00 Prague 8, Czech Republic
[d] *Los Alamos National Laboratory, Los Alamos, New Mexico 87545, USA*
[e] *Joint Institute for Nuclear Research, 141980 Dubna, Russia*
[f] *Nuclear Physics Institute, Czech Academy of Sciences, CZ-250 68 Řež, Czech Republic*
E-mail: mitchell@tunl.duke.edu

The γ rays following the ^{94,95}Mo(n,γ)Mo reactions have been studied by the time-of-flight method with the DANCE (Detector for Advanced Neutron Capture Experiments) array of 160 BaF_2 scintillation detectors at the Los Alamos Neutron Science Center. The targets were enriched samples. The γ-ray multiplicities and energy spectra for different multiplicities were measured in *s*- and *p*-wave resonances up to E_n = 10 keV for ^{94}Mo and up to E_n = 2 keV for ^{95}Mo. Preliminary analysis assigned definite spins and parities in ^{96}Mo for about 60% of the resonances, while tentative spins and parities were assigned for the rest of observed resonances. In ^{95}Mo the parities were determined for the observed resonances, confirming previously known assignments.

Workshop on Photon Strength Functions and Related Topics
June 17-20 2007
Prague, Czech Republic

*Speaker.

PoS(PSF07)001

1. Introduction

A classic problem in neutron resonance spectroscopy is the assignment of the total angular momentum for resonances formed on targets with non-zero spin. The γ-ray multiplicity method is an approach to determining the spins of neutron resonances that uses the spin dependence of (n,γ) spectra. The method was initiated in the 1960s by Coceva *et al.* [1] at the electron linac of the Institute for Reference Materials and Measurements at Geel, Belgium, and later was developed into multiplicity spectrometry by Muradyan *et al.* [2] at the Kurchatov Atomic Energy Institute in Moscow. The method was also applied at the Linac/Booster of the Joint Institute for Nuclear Research, Dubna [3] and at the RPI linac at Troy, NY [4]. At these institutions NaI(Tl) crystals were used as scintillation detectors of the γ-ray cascades originating from resonance neutron capture.

The advent of more sophisticated BaF_2 detector arrays for studies of radioactive and/or very small samples at the LANSCE spallation neutron source at Los Alamos and at the n_TOF facility at CERN opened new possibilities for the determination of spins and parities of neutron resonances. One key motivation was the improvement of the values of neutron and photon strength functions. The DANCE facility at Los Alamos National Laboratory is a 160 crystal array [5], while the n_TOF array [6] has 40 crystals of a larger size. Here we report on the measurement at DANCE of γ-ray multiplicities and energy spectra for the resonant reaction ^{94}Mo(n,γ)Mo^{95} up to E$_n$ = 10 keV and for the resonant reaction ^{95}Mo(n,γ)Mo^{96} up to E$_n$ = 2 keV.

Data for the molybdenum isotopes are important for nuclear reactor design since molybdenum is used in some uranium fuel elements. Molybdenum isotopes are also fission products; their capture cross sections are required for fuel cycle calculations. These isotopes are also of nuclear physics interest, since they belong to the mass region where strong 'nonstatistical' electric dipole transitions from *p*-wave capturing states to low-lying positive parity states have been observed and interpreted in the framework of the valence-neutron model (see Ref. [7] and references therein). The neutron capture cross sections for molybdenum isotopes for energies $3 < E_n < 90$ keV have been measured at the Oak Ridge Electron Linear Accelerator [8], and total cross sections were measured in several investigations – see the Atlas of Neutron Resonances by Mughabghab [9].

Prior to our work, an experimental study of γ-ray spectra from neutron resonance capture on natural Mo was performed in Ref. [1] using a multiplicity method based on the ratios of single and coincidence counting rates from γ-ray detectors. The spins of neutron *s*-wave resonances in the compound nuclei ^{95}Mo and ^{97}Mo were assigned up to E$_n \simeq 1.25$ keV; several *p*-wave resonances were identified. A recent study of the (n,α) reaction on ^{95}Mo neutron resonances [10] stressed the importance of spin values and in this target for determining a reliable set of α-widths.

Relatively strong *p*-wave resonances are known to be abundant in the atomic mass region A = 90 – 100; the *p*-wave neutron strength function in this region is about 10 times stronger than the *s*-wave neutron strength function. Therefore a significant number of negative parity resonances are expected. Parity evaluations for resonances in the Mo isotopes are reported in [9]. This evaluation (of the orbital angular momentum and therefore the parity of the resonance) is based on the separation of the statistical distributions of the reduced neutron widths of *s*- and *p*-wave resonances [11] with the use of Bayes' theorem on conditional probability. An independent experimental measurement of neutron resonance parities is important to supplement this probabilistic argument.

The multiplicity method is described in section 2.1, while modeling of the statistical γ-ray

cascade is described in section 2.2. The experimental method and the data processing are described in sections 3 and 4. The experimental results and analysis are presented in section 5, followed by a brief summary.

2. Gamma-Ray Multiplicities

2.1 Method

The γ-ray multiplicity method can be applied to those compound nuclei for which the neutron radiative capture can be described by the statistical model. Excluding magic nuclei, these are the medium-weight and heavy nuclei. The γ-ray multiplicity method consists of the measurement of the cascade gamma spectra after the de-excitation of the compound nucleus formed by neutron capture. The method is based on the systematics of probabilities for transitions of various multipolarities. Systematics of the photon strength functions (see e.g., Ref. [12]) indicate that except for transitions between low-lying levels, partial radiation widths of dipole (E1,M1) transitions are on average much larger than those of quadrupole (E2,M2) transitions and that the E1 transitions in heavy nuclei are usually an order of magnitude stronger than M1 transitions. Because of the dipole multipolarity, after each transition the difference between the spins of the initial and final states in a given transition is 0 or 1. The multiplicity M_J is defined as the average number of transitions (or photons) per cascade initiated from a resonance with spin J: $M_J = \sum k P_J(k) / \sum P_J(k)$. For s-wave neutron resonances the spin J has the values $J_+ = I + 1/2$ and $J_- = I - 1/2$. The average multiplicity is expected to be different for J_- than for J_+. This conjecture was established [1, 2, 3] by Monte Carlo simulations of the gamma-cascades following neutron capture. The J-spin effect on multiplicity, although not large for Mo, ($\Delta M_J / < M > \sim 7\%$), results in the separation of M_J values of s-wave resonances into two different groups, corresponding to the two possible spin values $J_+ = 3$ and $J_- = 2$. This can be measured reliably with an efficient detector such as DANCE. For p-wave resonances in ^{96}Mo the possible spins are 1, 2, 3, and 4, and the situation is more complicated. This is discussed in section 2.2.

Naturally, the spin of the neutron resonance should affect not only the multiplicity distributions (these are defined as the frequency spectra $P_J(k)$ of the number of photons, k, emitted in the cascades) and the average value M_J, but also the gross structure of the γ-energy spectrum $N_k(E_\gamma)$ from the k-fold cascades. In some cases the γ-ray energy spectra from neutron resonances depend significantly on the parity of the resonances. For the molybdenum compound nuclei the low-lying excited states up to $E_x \simeq 2.5$ MeV all have positive parities. In particular, the p-wave ($l = 1$) resonances in ^{94,95}Mo have negative parity and can decay to low-lying positive parity states by emitting high energy primary E1 γ-quanta, while the M1 transitions from s-wave ($l = 0$) resonances to the same low-lying states are on average less intense. Therefore, the prevalence of E1 primary high energy transitions to these low-lying states should be a signature of p-wave resonances. This fingerprint feature of the shape of primary gamma spectra should also hold for the shape of the k-fold (especially two-fold) coincidence gamma spectra. Therefore the shape of γ spectra was used for parity assignments of neutron resonances in molybdenum.

2.2 Modeling photon cascades

In order to support the general arguments of section 2.1, simulations for ^{94,95}Mo targets were

performed using the DICEBOX code [13]. In these simulations, the input consists of the experimental level energies, their spins and decay modes for the discrete part of the nuclear excitation spectrum below some value E_{crit}, and nuclear models for the level density $\rho(E_a, J_a^{\pi_a})$ and the photon strength functions (PSFs), f_{XL}, of a given multipolarity and electromagnetic type XL. The code includes options for the level density and the photon strength functions. Descriptions of these models are given in the literature, e.g., in Ref. [13].

The complete level scheme and their decay modes include both the quasi-continuum and discrete regions. The statistical cascade gamma-decay in the quasi-continuum region is simulated by the Monte Carlo technique. The levels above E_{crit} are generated by a random discritization of the chosen level density formula and also simulates the decay of all levels. For this last task the partial radiation widths for transitions between any levels a and b must be chosen. This is accomplished with the use of the formula

$$\Gamma_{ab} = \sum_{X,L} y_{XL}^2 (E_a - E_b)^{2L+1} \frac{f_{XL}(E_a - E_b)}{\rho(E_a, J_a^{\pi_a})}, \tag{2.1}$$

where y_{XL} is a randomly generated number from a normal distribution with zero mean and unit variance. [13]). This provides a simulation of the Porter-Thomas distribution of partial gamma widths. The combination of the levels generated and the transition probabilities between these levels is defined as one nuclear realization from the ensemble of possible decay schemes. Within each nuclear realization the code generates up to 50,000 cascade events populating statistically the known levels. Usually about 20 realizations are required in order to provide a statistically significant approximation for the cascade characteristics and to provide estimates of their fluctuations.

The simulation results (which depend on the spin of the final levels and on the models of the PSFs used) are listed in Table 1. The calculations were performed with the use of a constant temperature level density, the Kadmensky-Markushev-Furman (KMF) model for the PSF($E1$), single particle estimates for the PSF of other multipolarities, $E_{crit} = 2.5$ MeV and the γ-ray sum energy window from 7.6 $-$9.2 MeV (the calculated total radiative widths $\Gamma_\gamma^s = 154 \pm 8$ meV and $\Gamma_\gamma^p = 185 \pm 20$ meV agree with experimental values reported in [9]). For ^{95}Mo the simulations predict an absolute difference in average multiplicity of about 0.30 between resonances with spin differing by one. This trend for the difference is also reproduced when other models are used. Table 1 also provides information on the size of fluctuations in M_J due to the statistical nature of the γ-decay. Generally, p-wave resonances have larger fluctuations in their average multiplicity than s-wave resonances. One concludes that with the use only of average multiplicity values one can identify J^π equal to 1^- and 2^-. It is not possible to determine the resonance spin for the parity mixed groups of spins $(2^+, 3^-)$ and $(3^+, 4^-)$ from the average M value alone.

In order to to determine qualitatively whether it is possible to separate resonance parities (and therefore identify spins J inside the mixed groups) additional modeling was performed. We calculated, using DICEBOX with the same model parameters as above, the γ-ray energy spectra from the two-step cascades ending on the ground and first excited states of ^{96}Mo for the initial J$^\pi$ combinations $(2^+, 3^-)$ and $(3^+, 4^-)$. Fig. 1 presents an example of spectra for the ($J^\pi = 2^+$, $J^\pi = 3^-$) case. The shape of these two spectra is quite different – especially the pronounced bump in the middle

Table 1: Average multiplicity $< M_J >$ calculated for *s*- and *p*- wave resonances in ^{94}Mo- and ^{95}Mo-targets.

Quantity	$< M_J >$					
J	1/2	3/2	1	2	3	4
^{94}Mo, *s*-waves	3.25(4)					
^{94}Mo, *p*-waves	3.03(15)	3.07(15)				
^{95}Mo, *s*-waves				3.90(5)	4.23(7)	
^{95}Mo, *p*-waves			3.30(15)	3.68(20)	4.00(23)	4.30(25)

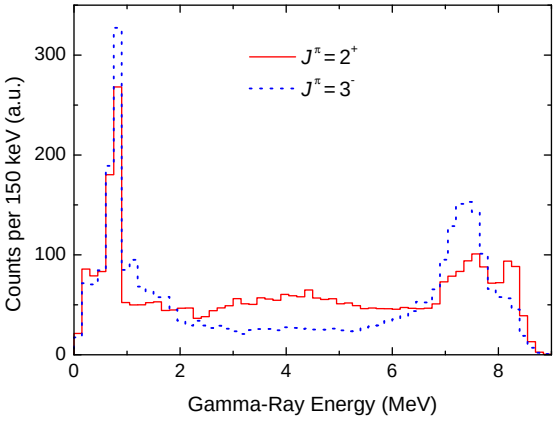

Figure 1: Calculated two-step cascade γ-ray energy spectra for *s*-wave resonances ($J^\pi = 2^+$) (full red line) and *p*-wave resonances ($J^\pi = 3^-$) (dotted blue line) in the ^{95}Mo$(n,\gamma)^{96}$Mo reaction. The size of the energy bins in the histograms is 150 keV.

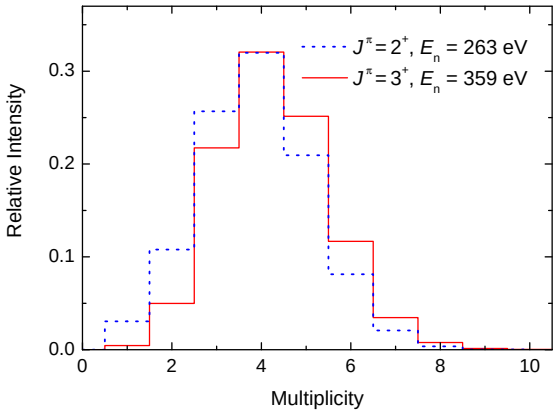

Figure 2: Multiplicity spectra for *s*-wave resonances at 263 eV ($J^\pi = 2^+$) and 359 eV ($J^\pi = 3^+$) in the ^{95}Mo(n,γ)^{96}Mo reaction.

part of the $J^\pi = 2^+$ spectrum and the strong peaks at the spectrum borders for the $J^\pi = 3^-$ case. The calculated spectra for $J^\pi = 3^+$ and $J^\pi = 4^-$ resonances have similar but weaker differences.

Analogous calculations for the ^{94}Mo target led to lower average multiplicity values (see Table 1) than for the ^{95}Mo target. They also show no appreciable sensitivity of $< M_J >$ to resonance spin, which in this case is either 1/2 or 3/2. The reason for this different behavior is that there are many low-lying states in the ^{95}Mo product nucleus (below 1 MeV) with J-values of 1/2, 3/2, 5/2, and 7/2 as compared to only one low-lying level in ^{96}Mo $(J = 2)$ in the first MeV. The two-step γ-ray cascades ending on these levels have different multiplicity values for a fixed initial spin, and when a mixture of such cascades is combined the sensitivity to the initial spin is averaged out. This happens with the DANCE detector and its broad energy resolution.

Nevertheless, the sensitivity of two-step cascade γ-ray spectra to the parity of neutron resonances in ^{94}Mo remains, similar to that observed for ^{95}Mo. This due to the different shapes of the γ-ray energy spectra with the same features as described above.

More elaborate modeling of n-step cascades and sum energy gamma-spectra for different theoretical models of the PSFs and inclusion of the γ-ray energy response of the DANCE detector system was also performed using the GEANT3 code [14, 15]. The details will be published else-

where. In the present paper we consider only the multiplicity two spectra, since they contain the most information on the spin and parity values of the neutron resonances in molybdenum.

3. Experimental setup and measurements

3.1 Experimental setup

The experiments were performed at the spallation neutron source of the Los Alamos Neutron Science Center (LANSCE) [16]. The 800-MeV H^- beam of about 625 ms duration from the LANSCE linac is converted to protons by thin foil stripping and injected into the proton storage ring. The injected beam is stacked on itself until protons from the entire linac macropulse are stored. This reduces the proton pulse width to about 125 ns full width at half maximum. This pulsed beam is extracted with a repetition rate of 20 Hz and transported to a tungsten spallation target, where fast neutrons are created. After passing through a water moderator, the moderated neutrons with a white energy spectrum enter evacuated flight paths. The DANCE detector array is installed on the 20-m neutron flight path 14 at the Manuel Lujan Jr. Neutron Scattering Center.

The DANCE spectrometer [5, 17] is a $\simeq 4\pi$ BaF_2 crystal array designed for studying neutron capture cross sections on small quantities of radioactive material or isotopic samples. The DANCE array consists of 160 BaF_2 scintillation crystals, which detect γ-rays following neutron capture. The array is highly segmented to reduce the high instantaneous count rate per detector. Each crystal has a length of 15 cm, with an inner radius of 17 cm for the ball. The area of each crystal facing the target is $\simeq$ 23 cm^2; the volume of each crystal is 734 cm^3. Neutrons scattered into the detector can be captured on the barium isotopes and produce an undesirable background. To reduce this background, a ^{6}LiH shell about 4-cm thick is placed between the sample and the BaF_2 crystals. The remaining background is subtracted in the off-line analysis; this subtraction procedure relies on the the calorimetric properties of the detector array (different Q-values and multiplicity distributions for Ba and Mo).

3.2 Measurements

Besides the BaF_2 crystals, the DANCE setup includes four more detectors: two silicon solid-state detectors looking at alpha and triton particles from a LiF foil, a uranium fission chamber, and a BF_3 proportional counter. All of these were used for monitoring the neutron flux and for obtaining the energy dependence of the flux. The Mo targets were two metal foils with a thickness of 50 mg/cm^2 for ^{94}Mo and of 25 mg/cm^2 for ^{95}Mo. The isotopic composition of the targets is listed in Table 2.

4. Data analysis

4.1 On-line data processing

The DANCE acquisition system [18] is based on waveform digitization of signals from all 160 barium fluoride detectors. The waveforms provide information on timing, particle type, and absorbed energy for each physical event in the crystals. Crystals are connected to Acqiris DC265

Table 2: Isotopic composition for the targets used in the measurements. The amount of isotope is listed as the percentage of the target material.

Target	Isotope abundances						
	^{92}Mo	^{94}Mo	^{95}Mo	^{96}Mo	^{97}Mo	^{98}Mo	^{100}Mo
^{94}Mo	0.73	91.59	5.35	1.11	0.37	0.65	0.20
^{95}Mo	0.26	0.63	96.47	1.45	0.46	0.63	0.15

digitizers through two channels able to handle both high and low amplitudes with a resolution of 8 bits at a sampling rate of 500 MHz. Each digitizer has 128 kbytes of fast memory per channel. The digitizers are arranged in 14 compact PCI crates with six digitizers per crate, one crate per 12 BaF_2 crystals. Each crate contains an embedded Intel based 1.8-GHz single board computer running the Linux operating system, and a front-end acquisition program written using the MIDAS (Maximum Integrated Data Acquisition System) framework [19]. Written without any selection, the DANCE typical raw data rate would be of the order of 1 Terabyte per hour, which is not practical. The problem with the disk space is bypassed by on-line partial processing of waveforms from digitizers using MIDAS. In this step information on the fast and slow parts of the signal is integrated and the integrals are stored instead of the whole waveforms; this leads to a compression factor of 20.

There are several options for data taking at DANCE. In this experiment the mode having a 3 μs dead-time was used. In this mode, use is made of NIM hardware to provide an external digitizer trigger whenever the energy deposited in crystals firing within a 100 nanosecond time window exceeds a preset energy threshold. This gate is called the 'crystal multiplicity' gate. The appropriate digitizers collect data where the gains for the two channels for a specific crystal differ by a factor of 10 in order to capture both the large amplitude fast peaks as well as the much lower amplitude of the slow decay component. This feature is used for discrimination against the α-background from the natural radioactivity of BaF_2 crystals, as described in [17]. All data from a given proton pulse are collected into one 'MIDAS event' on a disk.

4.2 Off-line data processing

The code ROME is based on the CERN ROOT [21] framework. Off-line data processing is performed with a dedicated code DANCE ANALYSER [18] written in the ROME framework. Because one MIDAS raw data event actually corresponds to many physics events, the primary analysis task,Extract Physics Events, analyzes a raw event and provides 'real' physics events to the next tasks; these consist of producing data calibrated in γ-ray energy and time-of-flight, and gating and graphing the data for producing raw count rates to calculate required physics quantities.

In particular, the extraction of the γ-ray multiplicity, the so-called 'cluster multiplicity', from the instrumental 'crystal multiplicity' is performed based on the timing and location characteristics of an event. The photons often do not deposit their full energy in one crystal. Therefore all contiguous crystals, that have fired during an event, are combined into one single cluster event. As a result the 'cluster multiplicity' is much closer to the true multiplicity of the gamma cascade than is the 'crystal multiplicity', which simply counts the total number of crystals that fire. The capture events in the off-line analysis were sorted by gates on the cluster multiplicity for each multiplicity

value and for each neutron resonance. The average value $< M >$ was calculated as :

$$< M >= \frac{\sum_{i=2}^{7} M_i C_i}{\sum_{i=2}^{7} C_i}, \tag{4.1}$$

where M_i and C_i are the multiplicities and counts for the corresponding multiplicity after subtracting background contributions. The M = 1 term has signifcant background and there are very few counts for M greater than 7.

The energy calibration of the DANCE crystals was performed with a combination of γ-ray sources: 662-keV from ^{137}Cs, 898-keV from ^{98}Y and 1275-keV from ^{22}Na and the intrinsic radioactivity of the detector material (^{226}Ra). The latter calibration was conducted on a run-by-run basis to provide the 'energy alignment' of all crystals in the off-line analysis. In the DANCE array there is also a time difference in the signals from individual crystals. A detailed description of the time calibration is given by Hatarik [22]. The achieved precision of 20 ns in time alignment was crucial for definition of a 'real' capture event in the off-line analysis.

Because of its nearly 4π geometry and high photon detection efficiency, the DANCE array is able to measure nearly the total reaction energy released in the neutron capture event, which is

$$E_{total} = B_n + E_n, \tag{4.2}$$

where B_n is the neutron binding energy in the compound nucleus and E_n is the center-of-mass kinetic energy of the neutron. In the off-line analysis, the γ-ray spectra were sorted by gates set on specific sum energy windows which were $7.6 - 9.2$ MeV for the ^{95}Mo target (B_n = 9.15 MeV) and $6.3 - 7.5$ MeV for the ^{94}Mo target (B_n = 7.36 MeV).

5. Experimental results

5.1 The ^{95}Mo$(n,\gamma)^{96}$Mo reaction

The yield of the detector array versus neutron energy for the ^{95}Mo target is shown in Fig. 3. The peaks are labeled by the resonance energy values taken from [9].

As an example of the measured multiplicity distributions for *s*-wave resonances with different spins, in Fig. 2 multiplicity spectra are shown for the 554-eV ($J = 2$) and 44.5-eV ($J = 3$) resonances. The average value is higher for the state with the higher *J* value. The average multiplicity values for all *s*-wave neutron resonances measured in the ^{95}Mo$(n,\gamma)^{96}$Mo reaction are shown in Fig. 4.

The *M* values are distributed into two distinct groups corresponding to spins $J = 2$ (lower line with $< M_J >= 3.93$) and $J = 3$ (upper line with $< M_J >= 4.23$). In obtaining this plot, it was crucial to separate *s*-wave resonances from *p*-wave resonances. This was achieved by the inspection of shapes of γ-ray energy spectra for multiplicity $M = 2$, as explained in Section IIB. A representative example of such spectra is shown in Fig. 5 for a pair of resonances: an *s*-wave resonance at 554 eV ($J = 2^+$) and a *p*-wave resonance at 708 eV ($J = 3^-$). As predicted by the modeling, the $J = 2^+$ spectrum is characterized by a bump near $E_\gamma = 4$ MeV. Spectra for other resonances follow this trend; they are compiled by Sheets in [15].

Table 3: Parameters of resonances in ^{95}Mo$(n,\gamma)^{96}$Mo reaction. DANCE results are compared with the compilation by Mughabghab. Multiplicity calculated from M=2-7.

Mughabghab				DANCE		
E [eV]	J	l	$2g\Gamma_n$ [meV]	$\langle$M$\rangle$	J^π	Comments
44.7	3	0	222±10	4.23(1)	3^+	
106.1				3.68(3)	$(1^-,2^-)$	New
110.4	1	1	0.18±0.04	3.36(1)	1^-	
117.8	2	(1)	0.26±0.04	3.73(1)	2^-	
159.5	3	0	16±1	4.20(1)	3^+	
218.3	(4)	1	2.0±0.2	3.72(1)	2^-	
245.8	(4)	(1)	0.48±0.07	4.02(2)	3^-	
263.3	(3)	(1)	1.6±0.2	3.96(1)	2^+	
324.0				3.66(2)	$(2,3^-)$	New
331.0	(2)	1	3.4±0.8	3.46(1)	1^-	
358.6	3	0	320±60	4.27(1)	3^+	
418.2	(2)	(1)	1.00±0.14	4.03(3)	3^-	
469.7	(2)	1	12±1	3.92(1)	2^+	
554.4	2	0	120±20	3.98(1)	2^+	
595.7	(3)	(1)	0.84±0.20	4.00(4)	3^-	
630.0	(4)	1	22±3	3.74(1)	2^-	
661.8	3	0	29±1	4.19(1)	$3^+(3^-)$	
680.2	3	0	830±50	4.27(1)	3^+	
702.8	(2)	(1)	2.9±0.3	4.10(2)	$(3^+,4^-)$	
708.3	(3)	(1)	13.3±0.8	4.00(1)	3^-	
745.5	(2)	1	7.9±2	3.87(2)	$3^-(2^-)$	
769.8	3	0	27±3	4.31(1)	3^+	
898.4	2	0	265±30	3.96(1)	2^+	
932.1	(1)	(1)	3.6±0.6	3.77(3)	2^-	
956.5	(1)	(1)	1.5±0.7	3.92(3)	$(1-3)^-$	
980.7	2	0	47±2.2	3.97(1)	2^+	
1011.1	(4)	1	12±1	3.93(1)	$2^-(1^-)$	
1023.8	3	0	130±20	4.27(1)	3^+	
1035.7	(4)	(1)	13±1	4.41(3)	$4^-(3^+)$	
1059.2	(3)	(1)	9.1±0.8	3.86(2)	$3^-(2^-)$	
1122.5	(1)	(1)	4.1±0.6	3.93(2)	$(1-3)^-$	
1144.6	2	0	250±50	3.97(1)	2^+	
1170.5	(2)	(1)	22.1±1.8	4.08(2)	3^-	
1203.4	3	0	221±9	4.29(1)	3^+	
1296.9	(4)	(1)	11±1	3.92(2)	$3^-(2^-)$	
1340.7	(2)	(0)	110±8	4.06(1)	3^-	
1360.6	(4)	(1)	5.9±0.8	4.10(4)	$(3,4^-)$	
1386.7	(2)	(1)	12±1	3.92(2)	$(2^-,3^-)$	
1419.3	(3)	(0)	620±70	4.23(1)	3^+	

Table 3: Continued

Mughabghab				DANCE		
E [eV]	J	l	$2g\Gamma_n$ [meV]	$\langle$M$\rangle$	J^π	Comments
1437.0	(3)	(1)	15±1.4	4.22(3)		weak
1495.5	(2)	(1)	160±40	3.92(1)	2^+	
1570.0	(3)	(1)	12±1	4.12(2)	$(1^-,2,3^-)$	weak
1576.8	(3)	(1)	10±0.8	4.23(2)	$(1^-,2,3)$	weak
1589.5	(3)	(0)	300±100	4.27(1)	3^+	
1677.4	(2)	(0)	360±50	4.29(1)	3^+	
1704.1	(3)	(1)	40.4±6.4	4.37(2)	$4^-(3^+)$	
1766.1	(3)	(0)	408±46	4.24(1)	3^+	
1788.0	(4)	(1)	55±10	4.40(2)	$4^-(3^+)$	
1841.7	(2)	(1)	39.0±5.2	3.93(2)	$3^-(2^-)$	
1853.3	(3)	(1)	6.4±0.8	3.84(3)	$(2^-,3^-)$	
1925.1	(2)	(1)	36.0±4.6	3.94(2)		weak
1950.2	(2)	(0)	390±110	3.97(1)	2^+	
1961.3	(3)	(1)	27±2.8	3.99(2)		weak
2048.1	(2)	(0)	241±100	3.90(1)	2^+	
2112.2	(2)	(1)	61±8	4.13(2)		weak
2130.1	(4)	(1)		4.24(2)	$3^+,(4^-)$	
2140.9	(4)	(1)	31.7±4.2	4.17(2)		weak

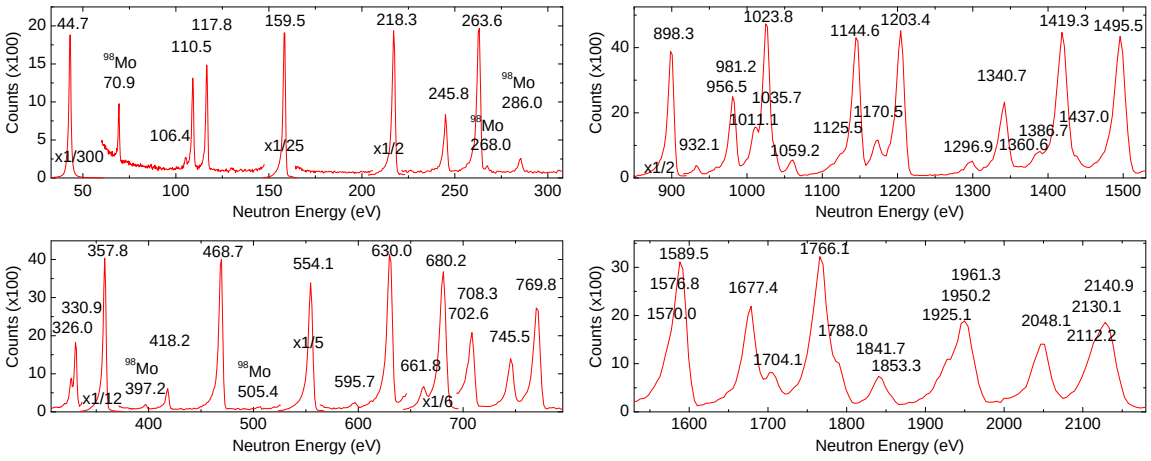

Figure 3: Neutron resonances in the ^{95}Mo$(n,\gamma)^{96}$Mo reaction: the DANCE detector yield versus neutron energy. The yield is the number of observed capture events per TOF channel with multiplicity $M > 1$ and a γ-ray sum energy from 7.6 to 9.2 MeV.

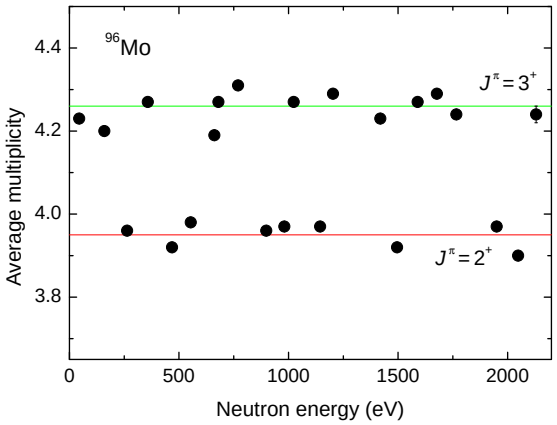

Figure 4: Multiplicities of *s*-wave neutron resonances from the ^{95}Mo$(n,\gamma)^{96}$Mo reaction in the neutron energy range from 40 to 2100 eV. Values along the lower line correspond to spin $J = 2$ and along the upper line to spin $J = 3$.

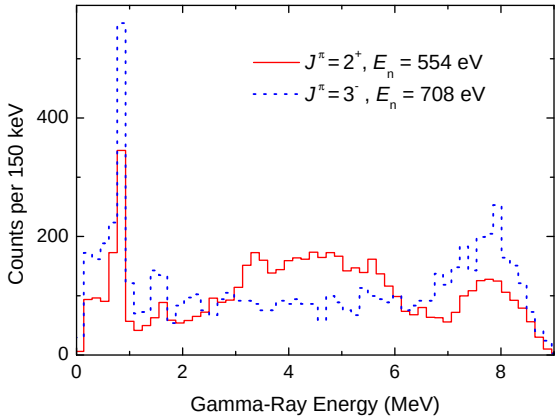

Figure 5: Measured γ-ray energy spectra for an *s*-wave resonance at 554 eV ($J^\pi = 2^+$) and a *p*-wave resonance at 708 eV ($J^\pi = 3^-$) in the ^{95}Mo$(n,\gamma)^{96}$Mo reaction. These spectra correspond to two-step cascades with the γ-ray sum energy window from 7.6 to 9.2 MeV.

After separating the *s*-wave resonances, the remaining multiplicity values were analyzed as *p*-wave resonances. Since the target ^{95}Mo spin is $J^+ = \frac{5}{2}^+$, *p*-wave capture leads to resonances with spins and parities of 1^-, 2^-, 3^-, and 4^-. As shown in simulations (see section 2.2), the average multiplicity values of neutron resonances in ^{95}Mo should depend on the resonance spin value. The calculated average multiplicity values are 3.30, 3.68, 4.00 and 4.30 for spins 1^-, 2^-, 3^-, and 4^-. The measured individual M_J-values fluctuate considerably. Unfortunately, the statistical accuracy for some resonances is not sufficient to make a spin assignment. Since the multiplicity separation into *J*-groups is not perfect, resonances that fall between groups were assigned a restricted range of spins.

The results of the spin/parity assignments of neutron resonances in the ^{95}Mo$(n,\gamma)^{96}$Mo reaction are listed in Table 3. One comment is in order: the resonance parity identification in Mo works only if the resonances are suffiently well separated.

5.2 The ^{94}Mo$(n,\gamma)^{95}$Mo reaction

The yield of the DANCE detector array versus neutron energy for the ^{94}Mo target is shown in Fig. 6. The peaks are labeled by the resonance energy values from [9].

The neutron binding energy in the compound nucleus ^{95}Mo is 7.37 MeV. The peak in the sum energy spectrum around this energy is asymmetric with an extended tail towards low energy. Therefore the analysis was restricted to events in the γ-ray sum energy window of 6.3 to 7.5 MeV, where the contribution from the background from neutron capture by ^{95}Mo admixture in the ^{94}Mo target and by Ba isotopes in the detector crystals was relatively small. This background was subtracted using the detector counts in the sum energy spectra above the energy of 7.5 MeV (the *Q*-values for the ^{135,137} Ba and ^{95}Mo isotopes are above 8.5 MeV). The background subtraction was especially important for this measurement because the strongest resonances in the ^{95}Mo$(n,\gamma)^{96}$Mo reaction

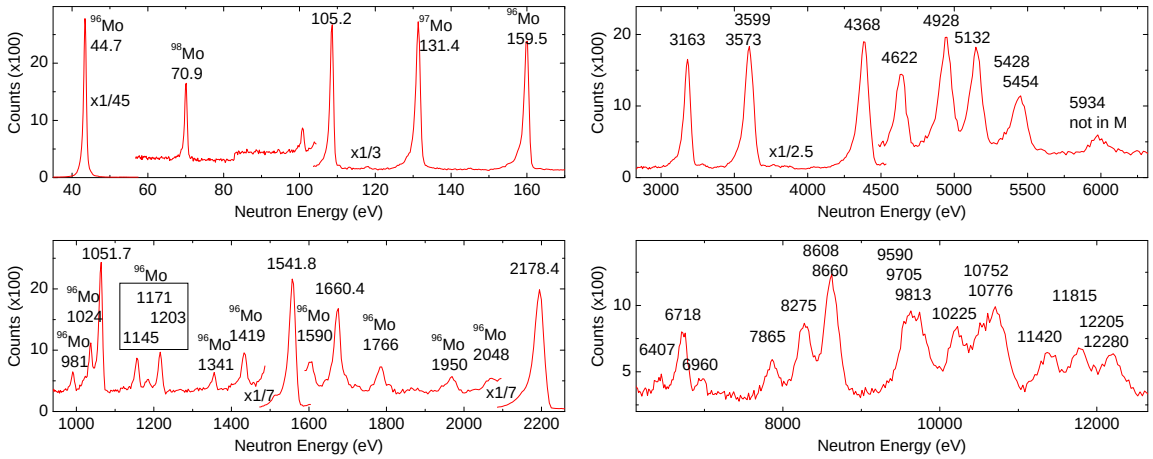

Figure 6: Neutron resonances in the ^{94}Mo$(n,\gamma)^{95}$Mo reaction: the DANCE detector yield is the number of observed capture events per TOF channel capture events with multiplicity $M > 1$ and the γ-ray sum energy window from 6.3 to 7.5 MeV.

are also the strongest ones in the ^{94}Mo target data. In general the ^{94}Mo resonances have significantly higher cross sections for scattering than the ^{95}Mo resonances. We excluded events with M = 1 from the determination of the average multiplicity, Eq. (4.1); most of the background due to neutron scattering in the detector leads to multiplicity one events.

The ground state of ^{94}Mo is 0^+; thus s-wave capture identifies directly the only possible spin and parity of $\frac{1}{2}^+$, while p-wave capture can excite resonances with $\frac{1}{2}^-$ and $\frac{3}{2}^-$. The ground state of the product nucleus ^{95}Mo is $\frac{5}{2}^+$ and that of the first excited state at 204 keV is $\frac{3}{2}^+$. There are several other excited levels that can contribute to the capture events with the sum energy in the chosen Q-window. The first excited negative parity levels with $J^\pi = (\frac{1}{2}^-$ and $\frac{3}{2}^-)$ are at 2214 and 2315 keV, respectively. As explained in section 2.2, this structure of the low-lying levels in ^{95}Mo (which is quite different from that in the ^{96}Mo product nucleus) removes the spin dependence of the observed average multiplicity for p-wave resonances.

An example of γ-ray energy spectra for the 3599-eV s-wave resonance and the 2178-eV p-wave resonance in ^{94}Mo$(n,\gamma)^{95}$Mo reaction is shown in Fig. 7. Spectra for other resonances [15] are similar to these. The resonances without a middle bump in the spectra are p-wave resonances. They have similar shapes and about the same average multiplicity. Thus spin assignments for the p-wave resonances ^{94}Mo cannot be made in this experiment.

Spectra of s-wave resonances have a clearly pronounced bump in the middle of the spectrum and the strongest of them have also a pair of lines at E_γ = 2.5 and 5 MeV. The latter evidently come from two-step transitions via the first negative parity levels near 2.5 MeV. The s-wave resonances are also distinguished by a higher average multiplicity value: $< M >= 3.25$, as compared with $< M >$ = 3.05 for the p-wave resonances.

The average multiplicity values for resonances in the neutron energy range from 100 eV to 10 keV measured in the ^{94}Mo$(n,\gamma)^{95}$Mo reaction are shown in Fig. 8. They are distributed in two groups corresponding to capture in p-wave (lower line with $< M >$ = 2.99) and s-wave (upper

Table 4: Parameters of resonances in ^{94}Mo$(n,\gamma)^{95}$Mo reaction. DANCE results are compared with the compilation by Mughabghab [9]. Multiplicities are now for M=2-7 and the detection threshold for γ rays was assumed to be 200 keV.

Mughabghab				DANCE		
E [eV]	J	l	$g\Gamma_n$ [meV]	$\langle M \rangle$	J^π	Comments
108.8		(1)	0.16±0.02	3.11(1)	$(^-)$	
278.5				3.22(3)	$1/2^+$	New ?
1051		(1)	6.1±0.6	3.00(1)	$^-$	
1542	1/2	0	1100±300	3.21(1)	$1/2^+$	
1660		(1)	12.4±1.7	3.01(1)	$^-$	
2178	3/2	1	383±135	2.98(1)	$^-$	
3163	(3/2)	(1)	244	2.97(1)	$^-$	
3573	(3/2)	(1)	260			Unresolved
3599	1/2	0	2500±500	3.17(1)	$1/2^+$	
4368	3/2	1	4000±1000	2.69(1)	$(^-)$	
4622	1/2	0	511±73	3.24(1)	$1/2^+$	
4928	(1/2)	(1)	1090±310	2.89(1)	$^-$	
5132	(3/2)	(1)	270	2.89(1)	$^-$	
5428	1/2	0	15300±2000	3.04(1)	$(^+)$	
5454		(1)	8±2			Unresolved
5934				2.90(2)	$^-$	
6407		(1)	30±8	3.10(3)	$^-$	
6718	(1/2)	(0)	1000±750	3.25(2)	$1/2^+$	
6960		(1)	31±8	2.93(3)	$^-$	
7128		(1)	9±2			Not found
7865	(1/2)	(0)	1000	3.25(2)	$1/2^+$	
8275	(3/2)	(1)	4000	3.05(2)	$^-$	
8608	3/2	(1)	1000	2.96(1)	$^-$	
8660		(1)	210			Unresolved
9590	(3/2)	(1)	1000	3.07(2)		
9705	(1/2)	(0)	500			Unresolved
9813		(1)	350	3.10(2)		
10225	(3/2)	(1)	6000±3000	3.04(2)	$^-$	

line with $< M >$ = 3.22) resonances. Since the statistical accuracy is limited, the definitive parity assignment was made based of the shapes of the γ-ray energy spectra. The final results of the parity assignments of neutron resonances in the ^{94}Mo$(n,\gamma)^{95}$Mo reaction are listed in Table 4. For all the observed resonances the previously known assignments are confirmed. The 4368-eV resonance has the lowest observed $< M >$ value, too small to be explained by statistical fluctuations. However, the γ-ray spectrum has a typical p-wave shape. The parity assignment of the 10225-eV resonance is based on its $< M >$ value, while the shape of the γ-ray spectrum indicates a contribution of positive parity resonances that probable originate from the unresolved triplet on its right wing. The 278.5

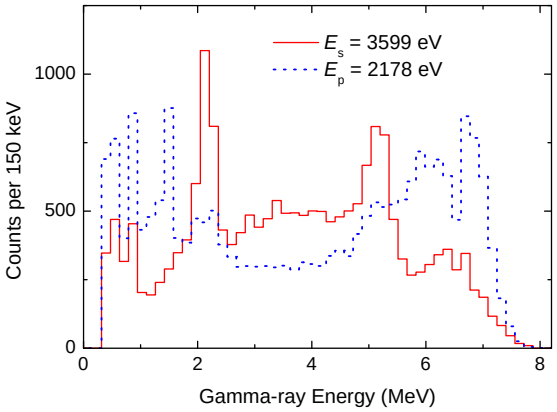

Figure 7: Measured γ-ray energy spectra for an *s*-wave resonance at 3599 eV and a *p*-wave resonance at 2178 eV in the ^{94}Mo$(n,\gamma)^{95}$Mo reaction. These spectra correspond to two-step cascades with the γ-ray sum energy window from 6.3 to 7.5 MeV.

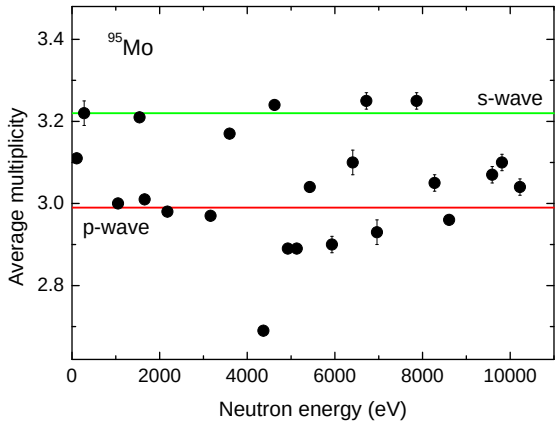

Figure 8: Multiplicities for neutron resonances from the ^{94}Mo$(n,\gamma)^{95}$Mo reaction in the neutron energy range from 100 eV to 10 keV. The *s*-wave and *p*-wave resonances have average M values of 3.22 and 2.99, respectively.

eV and 5934 eV resonances have not been previously observed and the locations of their Q-value peaks suggest that they belong to ^{94}Mo.

6. Summary and conclusion

Measurements of the γ-ray energy and multiplicity spectra following neutron resonance capture in isotopic ^{94}Mo and ^{95}Mo targets, were performed with the DANCE detector array at LANSCE by the time-of-flight method.

For the ^{95}Mo compound nucleus, the shape of gamma spectra in different resonances was used to determine resonance parities. For the observed resonances, all cases but one confirm previously known assignments. As expected, in the ^{94}Mo$(n,\gamma)^{95}$Mo reaction the difference between the average multiplicities of *p*-wave resonances was not large enough to use the multiplicity method for resonance spin assignments.

From the average multiplicity and spectral shape, spin and parity assignments were made for resonances in the ^{95}Mo$(n,\gamma)^{96}$Mo reaction below about 2 keV. The previously known indirect parity assignments were confirmed, and several new assignments were made. For *s*-wave resonances, the separation between the two M_J-value groups and the agreement of our results with those of other authors demonstrate the successful application of the multiplicity method with the DANCE detector array. For *p*-wave resonances in ^{95}Mo, where the separation of the different spin groups was not perfect due to a lack of statistical accuracy, the assignment of 23 spins from an ensemble of 35 *p*-wave resonances was made. Most of the results for the spins of the *p*-wave resonances are new.

Acknowledgments

This work was supported in part by the U. S. Department of Energy Grants No. DE-FG52-06NA26194 and No. DE-FG02-97-ER41042, and was performed under the auspices of the U. S.

Department of Energy by the University of California, Lawrence Livermore National Laboratory and Los Alamos National Laboratory under contract Nos. W-7405-ENG-48 and W-7405-ENG-36, respectively. This work has benefited from the use of the LANSCE accelerator facility, supported under DOE contract No. DE-AC52-06NA25396. It was also partly supported by the research plan MSM 0021620859 of the Ministry of Education of the Czech Republic.

References

[1] C. Coceva, F. Corvi, P. Giacobbe and G. Carraro, Nucl. Phys. A **117**, 586 (1968).

[2] G. V. Muradyan, Yu. V. Adamchuk, Yu. G. Shchepkin, and M. A. Voskanyan, Nucl. Sci. Eng. **90**, 60 (1985).

[3] G. Georgiev, Yu. S. Zamyatnin, L. B. Pikelner, G. V. Muradyan, Yu. V. Grigoriev, T. Madjarski, N. Janeva, Nucl. Phys. A **565**, 643 (1993).

[4] Shangwu Wang, M. Lubert, Y. Danon, N. C. Francis, R. C. Block, F. Bečvář and M. Krtička, Nucl. Instrum. Meth. Phys. Res. A **513**, 585 (2003).

[5] M. Heil, R. Reifarth, M. M. Fowler, R. Haight, F. Kaeppeler, R. S. Rundberg, E.H. Seabury, J. L. Ullmann, and M. K. Wisshak, Nucl. Instrum. Meth. Phys. Res. A **459**, 229 (2001).

[6] n_TOF Collaboration, Report INTC-2003-036, CERN, Switzerland, 2003.

[7] R. E. Chrien, G. W. Cole, G. G. Slaughter and J. A. Harvey, Phys. Rev. C **13**, 578 (1976).

[8] A. R. de L. Musgrove, B. J. Allen, J. W. Boldeman, and R. L. Macklin, Nucl. Phys. **A270**, 108 (1976).

[9] S. F. Mughabghab, *Atlas of neutron resonances* (Elsevier, Amsterdam, 2006).

[10] W. Rapp, P. E. Koehler, F. Käppeler, and S. Raman, Phys. Rev. C **68**, 015802 (2003).

[11] L. M. Bollinger and G. E. Thomas, Phys. Rev. **171**, 1293 (1968).

[12] C. M. McCullagh, M. L. Stelts, and R. E. Chrien, Phys. Rev. C **23**, 1394 (1981).

[13] F. Bečvář, Nucl. Instrum. Meth. Phys. Res. A **417**, 434 (1998).

[14] S. A. Sheets, U. Agvaanluvsan, M. Krtička, G. E. Mitchell, J. A. Becker, F. Bečvář and the DANCE Collaboration, in: *Capture Gamma-Ray Spectroscopy and Related Topics: 12-th International Symposium*, Editors A. Woehr and A. Aprahamian (American Institute of Physics, 2006), p. 597.

[15] S. A. Sheets, Ph.D. Thesis, North Carolina State University, 2007.

[16] P. W. Lisowski, C. D. Bowman, G. J. Russell, and S. A. Wender, Nucl. Sci. Eng., **106**, 208 (1990).

[17] R. Reifarth *et al.*, Nucl. Instrum. Meth. Phys. Res. A **531**, 530 (2004).

[18] J.M. Wouters *et al.*, IEEE Transactions on Nuclear Science, **53**, 880 (2006).

[19] S. Ritt and P. -A. Amaudruz, MIDAS − Maximum Integrated Data Acquisition System, http://midas.psi.ch.

[20] M. Schneebeli and S. Ritt, ROME − Root based Object Oriented Midas Extension (Online), http://midas.psi.ch/rome.

[21] ROOT Manual, http://root.cern.ch.

[22] R. Hatarik, Ph.D. Thesis, Colorado School of Mines, 2005.